Effects of postselected von Neumann measurement on the properties of single-mode radiation fields*

Yusuf Turek(玉素甫·吐拉克)†

School of Physics and Electronic Engineering, Xinjiang Normal University, Urumqi 830054, *China*

(Received 29 April 2020; revised manuscript received 20 May 2020; accepted manuscript online 23 June 2020)

Postselected von Neumann measurement characterized by postselection and weak value has been found to possess potential applications in quantum metrology and solved plenty of fundamental problems in quantum theory. As an application of this new measurement technique in quantum optics and quantum information processing, its effects on the features of single-mode radiation fields such as coherent state, squeezed vacuum state and Schrödinger cat sate are investigated by considering full-order effects of unitary evolution. The results show that the conditional probabilities of finding photons, second-order correlation functions, Q_m-factors and squeezing effects of those states after the postselected measurement is significantly changed are comparable with the corresponding initial pointer states.

Keywords: radiation field, postselection, weak value, statistical properties, squeezing parameter

PACS: 03.65.–w, 42.50.Ar, 42.50.–p, 03.65.Ta **DOI:** 10.1088/1674-1056/ab9f23

1. Introduction

Most researches in von Neumann type quantum measurement in recent years has focused on postseleceted weak measurement with sufficiently weak coupling between the measured system and pointer since it is useful to study the nature of the quantum world. This kind of postsselected weak measurement theory is originally proposed by Aharonov, Albert, and Vaidman in 1988,[1] and considered as a generalized version of standard von Neumann type measurement.[2] The result of weak coupling postselected weak measurement is called the "weak value", and generally is a complex number. One of the special feature of the weak value is that it can take the values which lie beyond the normal eigenvalue range of corresponding observable, and this effect will be very clear if the pre- and post-selected states are almost orthogonal. This feature of the weak value is called the signal amplification property of postselected weak measurement and its first weak signal amplification property experimentally demonstrated in 1991.[3] After that, it has been widely used to elucidate tremendous fundamental problems in quantum mechanics. For details about the weak measurement and its applications in signal amplification processes, we refer the readers to the recent overview of the field.[4,5] As we mentioned earlier, in postselected weak measurement the interaction strength is weak, and it is enough to consider up to the first-order evolution of a unitary operator for the whole measurement processes. However, if we want to connect the weak and strong measurement, check to clear the measurement feedback of postselected weak measurement and analyze experimental results obtained in nonideal measurements, the full order evolution of a unitary operator will be needed.[6–8] We call this kind of measurement the postselected von Neumann measurement. We know that in some quantum metrology problems, the precision of the measurement depends on measuring devices and requires to optimize the pointer states. The merits of postselected von Neumann measurement can be seen in pointer optimization schemes.

Recently, the state optimization problem in postselected von Neumann measurement has been presented widely, such as taking the Gaussian states,[4,9] Hermite–Gaussian or Laguerre–Gaussian states, and non-classical states.[10,11] The advantages of non-classical pointer states in increasing postselected measurement precision have been examined in recent studies.[10,12,13] Furthermore, in Ref. [14], the authors studied the effects of postselected measurement characterized by a modular value[15] to show the properties of semi-classical and non-classical pointer states considering the coherent, coherent squeezed, and Schrödinger cat state as a pointer. Since in their scheme the pointer operator is a projection operator onto one of the states of the basis of the pointer's Hilbert space and interaction strength only has taken one definite value, it cannot completely describe the effects of postselected measurement on the properties of the radiation field. However, to the knowledge of the author, the issue related to the study of the effects of postselected von Neumann measurement considering all interaction strengths to the inherent properties such as photon distribution, photon statistics, and squeezing effects of radiation field have not been handled and need to be investigated.

Furthermore, the above-mentioned properties of quantum radiation fields have many useful technological applications in quantum optics and quantum information processing such

*Project supported by the National Natural Science Foundation of China (Grant No. 11865017) and the Introduction Program of High-Level Talents of Xinjiang Ministry of Science, China.

†Corresponding author. E-mail:yusufu1984@hotmail.com

as single photon generation and detection,[16] gravitational wave detection,[17,18] quantum teleportation,[19–22] quantum computation,[23] generation and manipulation of atom–light entanglement,[24–26] and precision measurements,[27] etc. We know that the realization of these processes depends on the optimization of the related input quantum states such as coherent state,[28] squeezed state[29,30] and Schrödinger cat state.[31–33] As introduced in previous part, the postselected weak measurement technique has more advantages on signal optimization problem[34] and precision metrology[35–43] than traditional measurement theory. Thus, the investigation of the effects of postselected von Neumann measurement on the statistical and squeezing properties of radiation fields is worth studying to optimize the related quantum states to provide more effective methods for the implementation of the above-mentioned technological processes.

In this paper, motivated by the above-listed problems, we describe and examine the effects of postselected von Neumann measurement characterized by postselection and weak value on the properties of single-mode radiation fields. In order to achieve our goal, we choose the three typical states such as coherent state, squeezed vacuum state, and Schrödinger cat state as pointers and consider their polarization degree of freedom as a measured system, respectively. By taking full-order evolution of the unitary operator of our system, we separately study the photon distributions, statistical properties and squeezing effects of radiation fields and compare those with the initial state cases. To give more details about the effects of postselected von Neumann measurement on radiation fields, we plot more figures by considering all parameters that are related to the properties of those radiation fields, respectively. This study shows that the postselected measurement changes the properties of single-mode radiation fields dramatically for strong and weak measurement regimes with specific weak values. Especially the photon statistics and squeezing effect of coherent pointer state is too sensitive for the postselected von Neumann measurement processes.

This paper is organized as follows: In Section 2, we describe the model of our theory by brief reviewing the postselected von Neumann measurement and outline the tasks we want to investigate. In Section 3, we separately calculate exact analytical expressions of photon distribution, second-order correlation function, Mandel factor and squeezing parameter of those three-pointers by taking into account the full-order evaluation of unitary operator under final states given after postselected measurement finished and present our main results. Finally, we summarize our findings of this study in Section 4.

2. Model setup

To build up our model, we begin to review some basic concepts of the von Neumann measurement theory. The standard measurement consists of three elements; measured system, pointer (measurement device or meter) and environment, which induce the interaction between the system and the pointer. The description of the measurement process can be written in terms of Hamiltonian, and the total Hamiltonian of a measurement composed of three parts:[44]

$$H = H_{\rm s} + H_{\rm p(m)} + H_{\rm int}, \tag{1}$$

where $H_{\rm s}$ and $H_{\rm p(m)}$ represents the Hamiltonian of measured system and measuring device, respectively, and $H_{\rm int}$ is the interaction Hamiltonian between the measured system and the pointer. By considering the measurement efficiency and accuracy, in standard quantum measurement theory the interaction time between the system and the meter required to be too short so that the $H_{\rm s}$ and $H_{\rm p(m)}$ do not affect the final readout of the measurement result. Thus, in general, a measurement can only be described by the interaction part $H_{\rm int}$ of the total Hamiltonian, and it is taken to the standard von Neumann Hamiltonian as[2]

$$H_{\rm int} = g(t)\hat{A}\hat{P}, \quad \int_{t_0}^{t} g(t)\,{\rm d}t = g\delta(t-t_0), \tag{2}$$

where $\hat{A}$ represents the Hermitian operator corresponding to the observable of the system that we want to measure with $\hat{A}|\phi_n\rangle = a_n|\phi_n\rangle$, and $\hat{P}$ is the conjugate momentum operator to the position operator $\hat{X}$ of the pointer, i.e., $[\hat{X},\hat{P}] = {\rm i}\hat{I}$. The coupling $g(t)$ is a nonzero function in a finite interaction time interval $t-t_0$.

One can express the position $\hat{X}$ and momentum operator $\hat{P}$ of the pointer using the annihilation $\hat{a}$ and creation operator $\hat{a}^\dagger$ (satisfying $[\hat{a},\hat{a}^\dagger] = 1$) as[45]

$$\hat{X} = \sigma(\hat{a}^\dagger + \hat{a}), \tag{3}$$

$$\hat{P} = \frac{\rm i}{2\sigma}(\hat{a}^\dagger - \hat{a}), \tag{4}$$

where σ is the width of the beam. The Hamiltonian $H_{\rm int}$ can be rewritten in terms of a and $a^\dagger$ as $H_{\rm int} = \frac{{\rm i}g(t)}{2\sigma}\hat{A}(a^\dagger - a)$. If the Hermitian operator $\hat{A}$ satisfies the property $\hat{A}^2 = \hat{I}$, then the unitary evolution operator ${\rm e}^{-{\rm i}\int_{t_0}^{t} H_{\rm int}\,{\rm d}\tau}$ of our coupling system can be given by

$${\rm e}^{-{\rm i}g\hat{A}\otimes\hat{P}} = \frac{1}{2}(\hat{I}+\hat{A})\otimes D\left(\frac{s}{2}\right) + \frac{1}{2}(\hat{I}-\hat{A})\otimes D\left(-\frac{s}{2}\right), \tag{5}$$

where s is defined by $s :\equiv g/\sigma$, and $D\left(\frac{s}{2}\right)$ is a displacement operator and its expression can be written as $D(\frac{s}{2}) = {\rm e}^{\frac{s}{2}(\hat{a}^\dagger - \hat{a})}$. We must note that s characterizes the measurement strength, and $s \ll 1$ $(s > 1)$ corresponds to weak (strong) measurement regimes.

Assume that the system initially prepared in the state $|\psi_i\rangle$ and the initial pointer state is $|\phi\rangle$, then after interaction we project the state $\mathrm{e}^{-\mathrm{i}\int_{t_0}^{t} H_{\mathrm{int}}\,\mathrm{d}\tau}|\psi_i\rangle|\phi\rangle$ onto the postselected system state $|\psi_{\mathrm{f}}\rangle$, we can obtain the final state of the pointer. Furthermore, the normalized final state of the pointer can be written as

$$|\Phi\rangle = \mathcal{N}\left[\frac{1}{2}(\hat{I}+\langle A\rangle_w)\otimes D\left(\frac{s}{2}\right) + \frac{1}{2}(\hat{I}-\langle A\rangle_w)\otimes D\left(-\frac{s}{2}\right)\right]|\phi\rangle. \tag{6}$$

Here $\mathcal{N}$ is the normalization coefficient of $|\Phi\rangle$, and

$$\langle A\rangle_{\mathrm{w}} = \frac{\langle\psi_{\mathrm{f}}|\hat{A}|\psi_{\mathrm{i}}\rangle}{\langle\psi_{\mathrm{f}}|\psi_{\mathrm{i}}\rangle} \tag{7}$$

is called the weak value of Hermitian operator $\hat{A}$. From Eq. (6), we know that when the preselected state $|\psi_{\mathrm{i}}\rangle$ and the postselected state $|\psi_{\mathrm{f}}\rangle$ of the system are almost orthogonal, the absolute value of the weak value can be arbitrarily large and can be beyond the eigenvalue region of observable A. This feature leads to weak value amplification of weak signals and solving a lot of important problems in physics.

In this study, we take the transverse spatial degree of freedom of single-mode radiation field as pointer and its Hamiltonian $H_{\mathrm{m(p)}}$ is related to the generating processes of single mode radiation fields such as coherent state, squeezed vacuum state and Schrödinger cat state, etc. The polarization degree of freedom of single mode radiation field is taken to be the measured system, and its Hamiltonian H_{s} is related to the polarization of the beam. Based on the basic requirements of quantum measurement theory,[44] the H_{s} and $H_{\mathrm{m(p)}}$ do not affect our measurement results. Thus, in our current research, it is not necessary to give the explicit expressions of the system and meter in hereafter. We suppose that the operator to be observed is the spin x component of a spin-1/2 particle, i.e.,

$$A = \sigma_x = |\uparrow_z\rangle\langle\downarrow_z| + |\downarrow_z\rangle\langle\uparrow_z|, \tag{8}$$

where $|\uparrow_z\rangle$ and $\langle\downarrow_z|$ are eigenstates of the z-component of spin, σ_z, with the corresponding eigenvalues 1 and -1, respectively. We assume that the pre- and post-selected states of measured system are

$$|\psi_{\mathrm{i}}\rangle = \cos\frac{\theta}{2}|\uparrow_z\rangle + \mathrm{e}^{\mathrm{i}\varphi}\sin\frac{\theta}{2}|\downarrow_z\rangle, \tag{9}$$

and

$$|\psi_{\mathrm{f}}\rangle = |\uparrow_z\rangle, \tag{10}$$

respectively, and the corresponding weak value, Eq. (6), reads

$$\langle\sigma_x\rangle_{\mathrm{w}} = \mathrm{e}^{\mathrm{i}\varphi}\tan\frac{\theta}{2}, \tag{11}$$

where $\theta\in[0,\pi]$ and $\varphi\in[0,2\pi)$. In our system, the postselection probability is $P_{\mathrm{s}} = \cos^2\frac{\theta}{2}$. Note that throughout the rest of this study we will use this weak value for our purposes.

Furthermore, we take the initial pointer state $|\phi\rangle$ as a coherent state, squeezed vacuum state and Schrödinger cat state to study the effects of postselected measurement on the properties of those pointers, respectively. To achieve our goal:

(1) We study the conditional probability of finding n photons after postselected measurement. For the state $|\Phi\rangle$, the conditional probability of finding n photons can be calculated by

$$P_{\mathrm{post}}(n) = |\langle n|\Phi\rangle|^2, \tag{12}$$

and we compare it with the probability $P(n) = |\langle n|\phi\rangle|^2$ of initial pointer state $|\phi\rangle$.

(2) We investigate the second-order correlation function $g^{(2)}(0)$ and Mandel factor Q_{m} for the $|\Phi\rangle$ state. The second-order correlation function of a single-mode radiation field is defined as

$$g^{(2)}(0) = \frac{\langle a^\dagger a^\dagger aa\rangle}{\langle a^\dagger a\rangle^2}, \tag{13}$$

and the Mandel factor Q_{m} of the radiation field can be expressed in terms of $g^{(2)}(0)$ as

$$Q_{\mathrm{m}} = \langle n\rangle\left[g^{(2)}(0)-1\right]. \tag{14}$$

If $0\le g^{(2)}(0)<1$ and $-1\le Q_{\mathrm{m}}<0$ simultaneously, the corresponding radiation field has sub-Poissonian statistics and more nonclassical. We have mention that the quantity Q_{m} can never be smaller than -1 for any radiation field, and negative Q_{m} values, which are equivalent to sub-poissonian statistics, cannot be produced by any classical field.[46]

(3) We check the squeezing parameter of single-mode radiation field for the $|\Phi\rangle$ state. The squeezing parameter of the single-mode radiation field reads[47]

$$S_\phi = \langle :X_\phi^2: \rangle - \langle X_\phi\rangle^2, \tag{15}$$

where

$$X_\phi = \frac{1}{\sqrt{2}}\left(a\,\mathrm{e}^{-\mathrm{i}\phi} + a^\dagger\,\mathrm{e}^{\mathrm{i}\phi}\right), \quad [X_\phi, X_{\phi+\frac{\pi}{2}}] = \mathrm{i} \tag{16}$$

is the quadrature operator of the field, and :: stands for the normal ordering of the operator defined by $:aa^\dagger: = a^\dagger a$, whereas $aa^\dagger = a^\dagger a+1$. We can see that S_θ is related to the variance of X_θ, i.e.,

$$S_\phi = \left(\Delta X_\phi\right)^2 - \frac{1}{2}, \tag{17}$$

where $\Delta X_\phi = \sqrt{\langle X_\phi^2\rangle - \langle X_\phi\rangle^2}$. The minimum value of S_ϕ is $-1/2$ and for a nonclassical state $S_\phi\in[-1/2,0)$.

In the next section, we will study the above properties of three typical radiation fields by taking into the postselected measurement with arbitrary interaction strengths and weak values, respectively.

3. Effects of postselected measurement to typical single-mode radiation fields

In this section, we study the statistical properties and squeezing effects of typical single-mode radiation fields such as a coherent state, squeezed vacuum state and Schrödinger cat state, respectively, and compare the results with the corresponding initial state's case.

3.1. Coherent state

The coherent state is typical semi-classical, quadrature minimum-uncertainty state for all mean photon numbers. The coherent state was originally introduced by Schrödinger in 1926 as a Gaussian beam to describe the evolution of a harmonic oscillator,[48] and the mathematical formulation of coherent state (also called Glauber state) has been introduced by Glauber in 1963.[28] Coherent states play an important role in representing quantum dynamics, especially when the quantum evolution is close to classical.[49,50] Here we take the coherent state as initial pointer state[51]

$$|\alpha\rangle = D(\alpha)\,|0\rangle, \tag{18}$$

where $D(\alpha) = \mathrm{e}^{\alpha a^{\dagger} - \alpha^{*} a}$, and $\alpha = r\mathrm{e}^{\mathrm{i}\vartheta}$ is an arbitrary complex number. After unitary evolution given in Eq. (4), the total system state is post-selected to $|\psi_{\mathrm{f}}\rangle$, then we obtain the following normalized final state of coherent pointer state:

$$\begin{aligned}|\Psi\rangle \;=\; & \frac{\lambda}{\sqrt{2}}\left[(1+\langle A\rangle_{\mathrm{w}})\,\mathrm{e}^{-\mathrm{i}\frac{s}{2}\mathrm{Im}(\alpha)}\left|\alpha+\frac{s}{2}\right\rangle\right. \\ & \left.+(1-\langle A\rangle_{\mathrm{w}})\,\mathrm{e}^{\mathrm{i}\frac{s}{2}\mathrm{Im}(\alpha)}\left|\alpha-\frac{s}{2}\right\rangle\right],\end{aligned} \tag{19}$$

where the normalization coefficient is given as

$$\begin{aligned}\lambda^{-2} \;=\; & 1+|\langle A\rangle_{\mathrm{w}}|^2+\mathrm{e}^{-\frac{1}{2}s^2}(1+|\langle A\rangle_{\mathrm{w}}|^2 \\ & +2\mathrm{Re}\langle A\rangle_{\mathrm{w}})\cos(2s\,\mathrm{Im}(\alpha)),\end{aligned} \tag{20}$$

and Im (Re) represents the imaginary (real) part of a complex number.

The conditional probability of finding n photons after taking a postselected measurement for state $|\Psi\rangle$ is obtained from Eq. (11) by changing $|\Phi\rangle$ to a specific normalized state $|\Psi\rangle$. We plot the conditional probability of finding n photons under the normalized state $|\Psi\rangle$ and the analytical results are shown in Fig. 1. As indicated in Fig. 1, the black solid line represents the photon distribution probability for the initial state of coherent pointer state before postselected measurement, and it has a Poisson probability distribution. However, as shown in Fig. 1 the postselected measurement can change the photons Poisson distribution with increasing the weak value and changing the interaction strength s. Furthermore, from Fig. 1(a) we can know that $P_{\mathrm{coh}}(n)$ is larger, in the postslected case for some small photon number regions rather than the no interaction case.

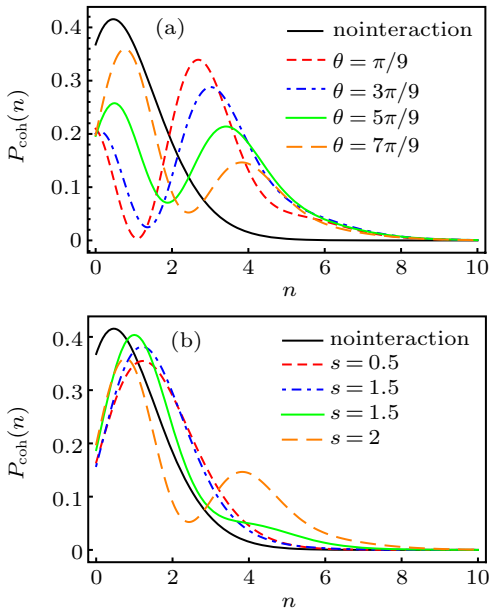

Fig. 1. Photon distribution $P_{\mathrm{coh}}(n)$ of coherent state as a function of photon number n for $\vartheta=\pi/3$, $\varphi=\pi/4$, $r=1$. (a) $P_{\mathrm{coh}}(n)$ plotted for $s=2$, and for various weak values ($\langle\sigma_x\rangle_{\mathrm{w}}=\mathrm{e}^{\mathrm{i}\pi/3}\tan\theta/2$) in the no interaction case (black curve). (b) $P_{\mathrm{coh}}(n)$ plotted for $\theta=7\pi/9$, and for various coupling strength s.

For coherent state $|\alpha\rangle$ (Eq. (17)) the second-order correlation function $g^{(2)}(0)$ is equal to one, i.e., $g^{(2)}(0)=1$ and the Mandel factor is equal to zero. Now we will calculate the $g^{(2)}_{\mathrm{coh}}(0)$ and $Q_{\mathrm{m,coh}}$ considering the final pointer state $|\Psi\rangle$ for the coherent pointer state. The expectation value of the photon number operator $\hat{n}=a^{\dagger}a$ under the state $|\Psi\rangle$ is

$$\begin{aligned}\langle n\rangle_{\Psi} \;=\; & \frac{|\lambda|^2}{4}\left\{|1+\langle A\rangle_{\mathrm{w}}|^2\left|\alpha+\frac{s}{2}\right|^2+|1-\langle A\rangle_{\mathrm{w}}|^2\left|\alpha-\frac{s}{2}\right|^2\right. \\ & +2\mathrm{e}^{-\frac{s^2}{2}}\mathrm{Re}[\mathrm{e}^{2\mathrm{i}s\mathrm{Im}(\alpha)}(1-|\langle A\rangle_{\mathrm{w}}|^2-2\mathrm{i}\,\mathrm{Im}\langle A\rangle_{\mathrm{w}}) \\ & \left.\times\left(\alpha+\frac{s}{2}\right)^{*}\left(\alpha-\frac{s}{2}\right)\right]\Big\}.\end{aligned} \tag{21}$$

If we take $s=0$, then $\langle n\rangle_{\mathrm{s=0}}=|\alpha|^2$. This is the photon number for the initial coherent state $|\alpha\rangle$. We can also obtain the expectation value of $\langle a^{\dagger 2}a^2\rangle$ as

$$\begin{aligned}\langle a^{\dagger 2}a^2\rangle_{\Psi} \;=\; & \frac{|\lambda|^2}{4}\left\{|1+\langle A\rangle_{\mathrm{w}}|^2\left|\alpha+\frac{s}{2}\right|^4+|1-\langle A\rangle_{\mathrm{w}}|^2\left|\alpha-\frac{s}{2}\right|^4\right. \\ & +2\mathrm{e}^{-\frac{s^2}{2}}\,\mathrm{Re}\left[\mathrm{e}^{2\mathrm{i}s|\alpha|\sin\phi}(1+\langle A\rangle^{*}_{\mathrm{w}})(1-\langle A\rangle_{\mathrm{w}})\right. \\ & \left.\left.\times\left(\alpha+\frac{s}{2}\right)^{*2}\left(\alpha-\frac{s}{2}\right)^{2}\right]\right\}.\end{aligned} \tag{22}$$

If we take $s=0$, it will give the value under the initial state $|\alpha\rangle$, i.e., $\langle a^{\dagger}a^{\dagger}aa\rangle_{\mathrm{s=0}}=|\alpha|^4$. By substituting the above expressions to Eqs. (12) and (13), we obtain the concrete expressions of $g^{(2)}_{\mathrm{coh}}(0)$ and $Q_{\mathrm{m,coh}}$. To investigate the effect of postselected measurement on the photon statistical properties of coherent state we plot the analytical figures of $g^{(2)}_{\mathrm{coh}}(0)$ and $Q_{\mathrm{m,coh}}$, and the results are shown in Fig. 2.

From Fig. 2 we can deduce that in postselected weak measurement region with large weak values (see the curves in Figs. 2(b) and 2(c)), the final state of the pointer state possesses sub-Poisson statistics ($0 < g^{(2)}(0) < 1$ and $-1 < Q_{\rm m} < 0$). From Fig. 2(d), we can see that in strong postselected measurement, the system has super Poisson statistics ($g^{(2)}(0) > 1$ and $Q_{\rm m} > 0$). Thus, the results summarized in Fig. 2 confirm that the postselected measurement can change the statistical properties of the coherent state significantly.

Since the coherent state is a minimum uncertainty state, there is no squeezing effect for coherent state $|\alpha\rangle$, i.e., $S_\phi = 0$. Next, we investigate the squeezing parameter $S_\phi^{\rm coh}$ for $|\Psi\rangle$ of the coherent pointer state. The expectation value of $X_{\phi,{\rm coh}}$ under the state $|\Psi\rangle$ is given by

$$\langle X_{\phi,{\rm coh}}\rangle_\Psi = \frac{|\lambda|^2}{\sqrt{2}}\Big\{(1+|\langle A\rangle_{\rm w}|^2)|\alpha|\cos(\phi-\theta)+s\cos\phi\,{\rm Re}[\langle A\rangle_{\rm w}]+\frac{1}{2}{\rm e}^{-\frac{1}{2}s^2}\,{\rm Re}[{\rm e}^{2is{\rm Im}(\alpha)}(1-\langle A\rangle_{\rm w})(1+\langle A\rangle_{\rm w}^*)$$
$$\times(2r\cos(\vartheta-\phi)+is\sin\phi)\Big]. \tag{23}$$

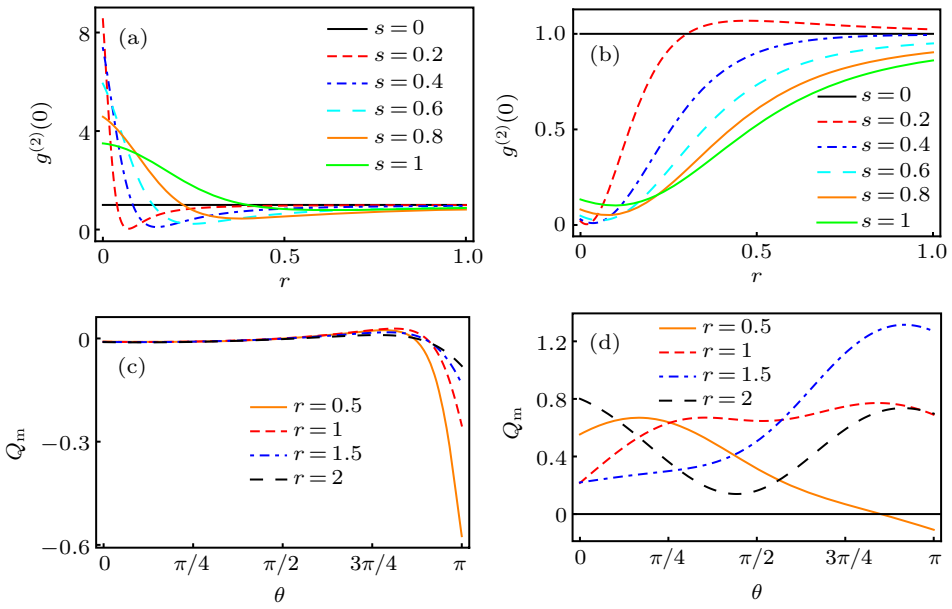

Fig. 2. Second-order correlation function $g^{(2)}_{\rm coh}(0)$ and Mandel factor $Q_{\rm m,coh}$ for the coherent state after postselected measurement. Here $\varphi = 4\pi/5$, $\vartheta = \pi/3$. $g^{(2)}_{\rm coh}(0)$ vs. coherent state parameter r for different interaction strength s (black sold line represents the initial coherent state $|\alpha\rangle$) and for (a) $\theta = \pi/3$, or (b) $\theta = 7\pi/9$. The Mandel factor $Q_{\rm m,coh}$ plotted as a function of the weak value for different r of coherent state and for (c) $s = 0.2$, or (d) $s = 2$.

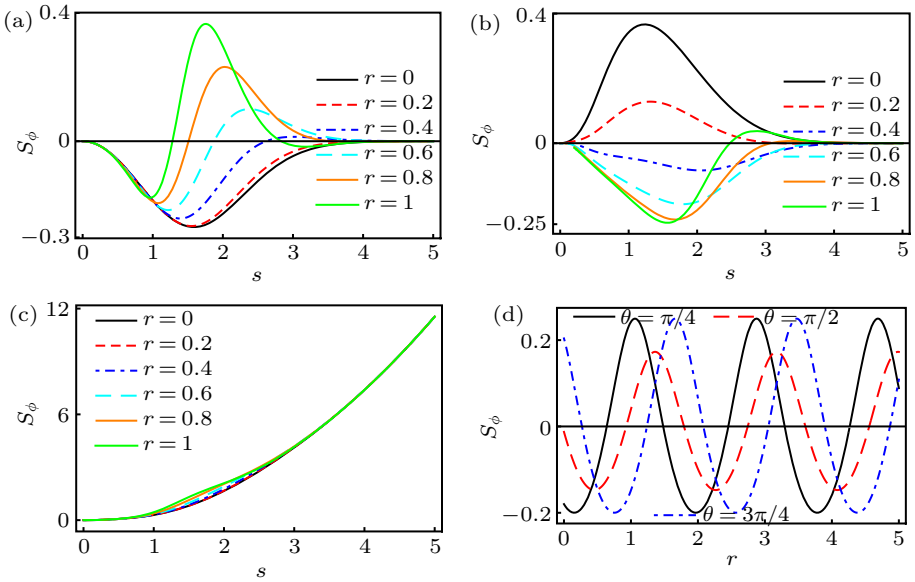

Fig. 3. The squeezing parameter $S_{\phi,{\rm coh}}$ for the coherent state after postselected measurement. Here $\varphi = 4\pi/5$, $\vartheta = \pi/3$. $S_{\phi,{\rm coh}}$ vs. interaction strength s for various r and P quadrature of the coherent state ($\phi = \pi/2$), but with different weak values: (a) $\theta = \pi/9$, (b) $\theta = 7\pi/9$. (c) $S_{\phi,{\rm coh}}$ plotted as a function of interaction strength s for various r and for $\theta = \pi/9$, $\phi = 0$ (represents the X quadrature of coherent state). (d) $S_{\phi,{\rm coh}}$ vs. coherent state parameter r for different weak values and for $\phi = \pi/2$, $s = 2$.

If $s=0$, then the above expression will reduce to the expectation value of X_ϕ under the initial coherent pointer state $|\alpha\rangle$, i.e., $\langle X_{\phi,\mathrm{oh}}\rangle_{\mathrm{s}=0}=\mathrm{Re}[\alpha\mathrm{e}^{-\mathrm{i}\phi}]$. The expectation value of $X^2_{\phi,\mathrm{coh}}$ with $|\Psi\rangle$ is given by

$$\begin{aligned}\langle X^2_{\phi,\mathrm{coh}}\rangle_\Psi &= \frac{1}{2}\langle(a\mathrm{e}^{-\mathrm{i}\phi}+a^\dagger\mathrm{e}^{\mathrm{i}\phi})(a\mathrm{e}^{-\mathrm{i}\phi}+a^\dagger\mathrm{e}^{\mathrm{i}\phi})\rangle\\ &= \frac{1}{2}\left[\langle a^2\rangle\mathrm{e}^{-2\mathrm{i}\phi}+\langle a^{\dagger 2}\rangle\mathrm{e}^{2\mathrm{i}\phi}+2\langle a^\dagger a\rangle+1\right]\\ &= \frac{1}{2}\left[2\mathrm{Re}[\langle a^2\rangle\mathrm{e}^{-2\mathrm{i}\phi}]+2\langle n\rangle+1\right],\end{aligned}\tag{24}$$

where

$$\begin{aligned}\langle a^2\rangle &= \frac{|\lambda|^2}{4}\Bigg\{|1+\langle A\rangle_\mathrm{w}|^2\left(\alpha+\frac{s}{2}\right)^2\\ &\quad+|1-\langle A\rangle_\mathrm{w}|^2\left(\alpha-\frac{s}{2}\right)^2\\ &\quad+\mathrm{e}^{2is\mathrm{Im}(\alpha)}\mathrm{e}^{-\frac{s^2}{2}}(1-\langle A\rangle_\mathrm{w})(1+\langle A\rangle^*_\mathrm{w})\left(\alpha-\frac{s}{2}\right)^2\\ &\quad+\mathrm{e}^{-2is\mathrm{Im}(\alpha)}\mathrm{e}^{-\frac{s^2}{2}}(1+\langle A\rangle_\mathrm{w})(1-\langle A\rangle^*_\mathrm{w})\left(\alpha+\frac{s}{2}\right)^2\Bigg\}.\end{aligned}\tag{25}$$

The squeezing parameter $S_{\phi,\mathrm{coh}}$ of state $|\Psi\rangle$ can be obtained by substituting Eqs. (23) and (24) into Eq. (17), and its analytical results are given in Fig. 3.

We can observe from Fig. 3 that after postselected measurement the squeezing parameter of the initial coherent state changes dramatically, and we can see the phase-dependent squeezing effect. The X quadrature ($\phi=0$) of the final state is not squeezed (see Fig. 3(c)), but P quadrature ($\phi=\frac{\pi}{2}$) of the final state has a squeezing effect for moderate interaction strengths (see Figs. 3(a), 3(b), and 3(d)) with any weak values.

3.2. Squeezed vacuum state

Our second pointer state is the squeezed vacuum state. Squeezed states of the radiation field are generated by degenerate parametric down-conversion in an optical cavity.[52] The squeezed state have important applications in many quantum information processing tasks, including gravitational wave detection,[17,18] quantum teleportation.[19,20] Suppose that a measuring device can be initially prepared in the squeezed vacuum state[51] defined by

$$|\xi\rangle=S(\xi)|0\rangle,\tag{26}$$

where $S(\xi)=\exp(\frac{1}{2}\xi^*a^2-\frac{1}{2}\xi a^{\dagger 2})$, and $\xi=\eta\mathrm{e}^{\mathrm{i}\delta}$ is an arbitrary complex number with modulus η and argument $\delta\in[0,2\pi]$. As indicated in Eq. (26), the squeezed vacuum state is generated by the action on the vacuum state $|0\rangle$ of the squeezing operator $S(\xi)$. After the postselected measurement processes as outlined in Section 2, the normalized final pointer state can be written as

$$|\varphi\rangle=\frac{\kappa}{2}\left[(1+\langle A\rangle_\mathrm{w})\left|\xi,\frac{s}{2}\right\rangle+(1-\langle A\rangle_\mathrm{w})\left|\xi,-\frac{s}{2}\right\rangle\right],\tag{27}$$

where the normalization coefficient κ is given by

$$\begin{aligned}\kappa &= \sqrt{2}\Bigg[1+|\langle A\rangle_\mathrm{w}|^2+(1-|\langle A\rangle_\mathrm{w}|^2)\\ &\quad\times\exp\left(-\frac{1}{2}s^2|\cosh\eta+\mathrm{e}^{\mathrm{i}\delta}\sinh\eta|^2\right)\Bigg]^{-\frac{1}{2}}\end{aligned}\tag{28}$$

and we note that $|\xi,\pm\frac{s}{2}\rangle=D(\pm\frac{s}{2})S(\xi)|0\rangle$ is a squeezed coherent state.

The probability amplitude of finding n photons in a squeezed coherent state is given by

$$\begin{aligned}&\langle n|\pm\frac{s}{2},\xi\rangle\\ &=\frac{1}{\sqrt{\cosh\eta}}\exp\left[-\frac{1}{2}\left|\pm\frac{s}{2}\right|^2-\frac{1}{2}\left(\pm\frac{s}{2}\right)^{*2}\mathrm{e}^{\mathrm{i}\delta}\tanh\eta\right]\\ &\quad\times\frac{\left(\frac{1}{2}\mathrm{e}^{\mathrm{i}\delta}\tanh\eta\right)^{\frac{n}{2}}}{\sqrt{n!}}H_n\left[\chi\left(\mathrm{e}^{\mathrm{i}\delta}\sinh(2r)\right)^{-\frac{1}{2}}\right]\end{aligned}\tag{29}$$

with $\chi=\pm\frac{s}{2}\cosh\eta+(\pm\frac{s}{2})^*\mathrm{e}^{\mathrm{i}\delta}\sinh\eta$. To find the conditional probability of n photons under the state $|\varphi\rangle$, we can use Eq. (12) by changing $|\Phi\rangle$ to $|\varphi\rangle$, and use Eq. (29). The effects of postselected measurement to the probability of finding n photons for state $|\varphi\rangle$ is displayed in Fig. 4. The black thick curve in Fig. 4(a) corresponds to the conditional photon probability for the initial pointer state $|\xi\rangle$. As illustrated in Fig. 4, the postselected measurement can change the photon distribution of the field, and in fewer photon number region the $P_\mathrm{sq}(n)$ with the state $|\varphi\rangle$ is larger than the no interaction case (see Fig. 4(a)). For definite squeeze parameter η and weak

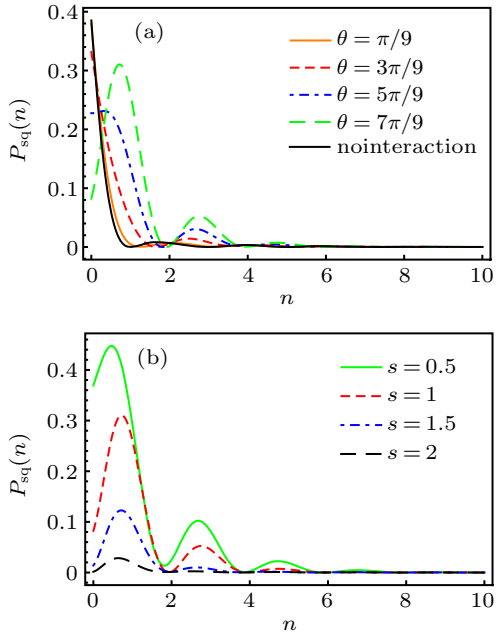

Fig. 4. Photon distribution $P_\mathrm{sq}(n)$ of squeezed vacuum state after postselected measurement as a function of n. Here $\delta=\pi/3$, $\varphi=\pi/3$, $\eta=0.5$. (a) $P_\mathrm{sq}(n)$ is plotted for $s=1$, and for the no interaction case (black curve) and various weak values. (b) $P_\mathrm{sq}(n)$ is plotted for $\theta=7\pi/9$, and for various interaction strength s.

measurement region ($s < 1$) with large weak values, P_{qs} is larger than strong measurement region ($s > 1$), but its occurrence probability is small.

The second-order correlation function $g^{(2)}(0)$ and the Mandel factor $Q_{\rm m}$ of the initial squeezed vacuum pointer state $|\xi\rangle$ is given by

$$g^{(2)}(0) = 3 + \frac{1}{\sinh^2\eta} \tag{30}$$

and

$$Q_{\rm m} = 1 + 2\sinh^2\eta, \tag{31}$$

respectively. It is clear that the number fluctuations of the squeezed vacuum pointer state initially are super-Poissonian, and for all values of η both $g^{(2)}(0)$ and $Q_{\rm m}$ cannot take the values to possess the sub-Poissonian statistics, which is a nonclassical property of the field. Now, we study the effect of postselected measurement to $g^{(2)}(0)$ and $Q_{\rm m}$ of the squeezed vacuum pointer state under the normalized final pointer state $|\varphi\rangle$. The expectation value of the photon number operator $a^\dagger a$ and the $(a^\dagger a)^2$ under the final state $|\varphi\rangle$ can be calculated, and their explicit expressions are given in Appendix A (since the expressions are too cumbersome to write here, we display them in the Appendix).

The analytical results for $g_{\rm sq}^{(2)}(0)$ and $Q_{\rm m,sq}$ under the state $|\varphi\rangle$ are presented in Fig. 5. It can be observed from Figs. 5(a) and 5(c) that both $g_{\rm sq}^{(2)}(0)$ and $Q_{\rm m,sq}$ can take the values, in which only sub-Poisson radiation field can possess the region $s \gtrsim 0.5$ for large weak values. For definite measurement strength s and larger weak value, the value $g_{\rm sq}^{(2)}(0)$ is lower than one and the value of $Q_{\rm m,sq}$ is less than zero when the squeezed state parameter η is less than one (see Figs. 5(b) and 5(d)). Thus, it is apparent that the postselected measurement dramatically changes the photon statistical properties of the initial squeezed pointer state $|\xi\rangle$.

The squeezing parameter S_ϕ of the initial squeezed vacuum state $|\xi\rangle$ can be calculated using Eqs. (14)–(16) and (33), and written as

$$S_\phi = \frac{1}{2}\left[\cosh^2\eta - \sinh(2\eta)\cos(2\phi - \delta) + \sinh^2\eta\right] - \frac{1}{2}. \tag{32}$$

It is evident from Eq. (32) that the squeezing effect of the squeezed vacuum state is phase-dependent: (i) If $\phi = \frac{\delta}{2}$, then $S_\phi = -\frac{1}{2}(1 - {\rm e}^{-2\eta})$, it has squeezing effect for $\eta > 0$. (ii) If $\phi = \frac{\delta}{2} + \frac{\pi}{2}$, then $S_\phi = \frac{1}{2}({\rm e}^{2\eta} - 1)$, there is no squeezing effect. This reveals that it spreads out the quadrature $X_{\phi=\frac{\delta}{2}}$ and at the same time squeezes the quadrature $X_{\phi=\frac{\delta}{2}+\frac{\pi}{2}}$.

The squeezing parameter $S_{\phi,sq}$ of the final normalized state $|\varphi\rangle$ after postselected von-Nuemann measurement can be calculated as the same processes of the initial state $|\xi\rangle$, and the analytical results are shown in Fig. 6. According to Figs. 6(a) and 6(b), the postselected measurement would have a negative effect on the squeezing effect of the squeezed vacuum state since $S_{\phi,sq}$ gradually becomes larger with increasing the measurement strength s. However, as indicated in Fig. 6(c), in weak measurement regime where $0 < s < 1$, the postselected measurement still has the effects on squeezing of the squeezed vacuum pointer state. As mentioned above the squeezing effect of the squeezed vacuum state is phase-dependent, and the postselected measurement has no positive effect on the squeezing of $X_{\phi=\frac{\pi}{2}}$ quadrature (see Fig. 6(d)).

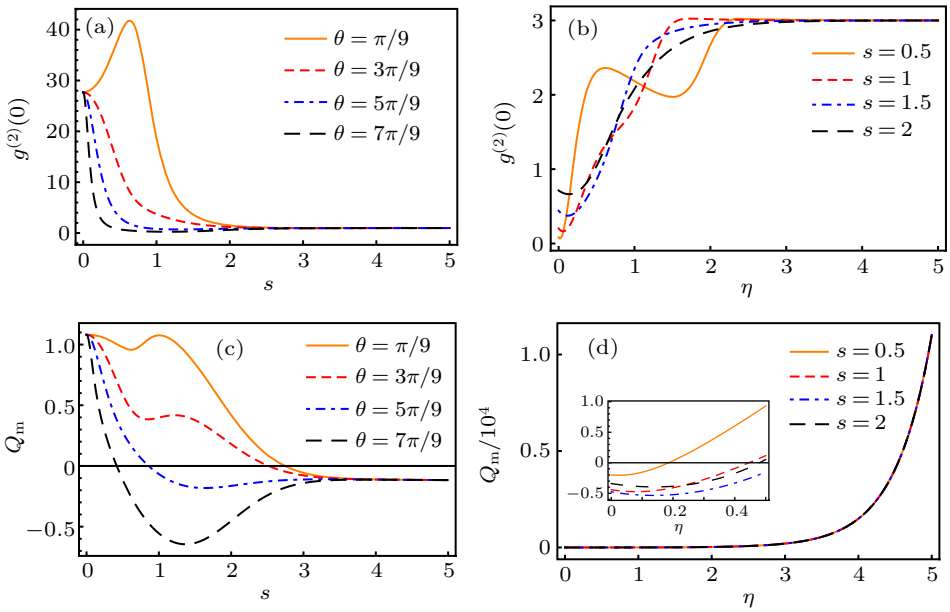

Fig. 5. Second-order correlation function $g_{\rm sq}^{(2)}(0)$ and the Mandel factor $Q_{\rm m,sq}$ of the squeezed vacuum state after postselected measurement. Here $\varphi = \pi/3$, $\delta = \pi/3$: (a) $g_{\rm sq}^{(2)}(0)$ vs. interaction strength s for different weak values and for $\eta = 0.2$; (b) $g_{\rm sq}^{(2)}(0)$ plotted as a function of squeezed vacuum state parameter η for various interaction strengths and for $\theta = 7\pi/9$; (c) $Q_{\rm m,sq}$ vs. interaction strength s for different weak values and for $\eta = 0.2$; (d) $Q_{\rm m,sq}$ plotted as a function of squeezed vacuum state parameter η for various interaction strengths and for $\theta = 7\pi/9$. Inset: the enlarged curves in the interval $\eta \in [0, 0.5]$.

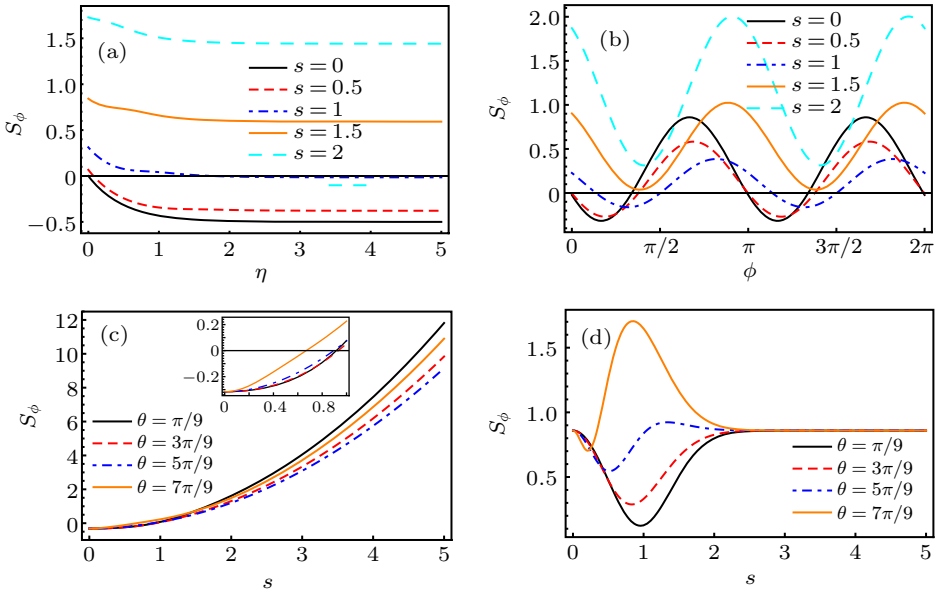

Fig. 6. Squeezing parameter $S_{\phi,sq}$ of the squeezed vacuum state after postselected measurement. Here $\varphi=\pi/3$. (a) S_ϕ vs. η of the squeezed vacuum state for different interaction strength s and for $\delta=\phi=0$, $\theta=\pi/9$. (b) $S_{\phi,sq}$ plotted as a function of ϕ for various interaction strength s and for $\eta=0.5$, $\delta=\pi/3$, and $\theta=\pi/9$. $S_{\phi,sq}$ vs. interaction strength s for different weak values and for $\delta=0$ and $\eta=0.5$, but with different ϕ: (c) $\phi=0$, (d) $\phi=\frac{\pi}{2}$. Inset: the enlarged curves in the interval $s\in(0,1]$.

3.3. Schrödinger cat state

In the above two subsections, we have already confirmed that postselected measurement characterized by a weak value can really change the statistical and squeezing effect of single-mode radiation fields. To further increase the reliability of our conclusions, in this subsection, we check the same phenomena by taking the Schrödinger cat state as a pointer. Schrödinger's cat is a gedanken experiment in quantum physics, proposed by Schrödinger in 1935,[53] and its corresponding state is called the Schrödinger cat state. The Schrödinger cat state plays significant roles not only in fundamental tests of quantum theory,[54–57] but also in many quantum information processing such as quantum computation,[23] quantum teleportation,[21,22] and precision measurements.[27] The Schrödinger cat state is composed by the superposition of two coherent correlated states moving in the opposite directions, and defined as[47]

$$|\Theta\rangle = K\left(|\alpha\rangle + \mathrm{e}^{\mathrm{i}\omega}|-\alpha\rangle\right), \tag{33}$$

where

$$K = \left[2+2\,\mathrm{e}^{-2|\alpha|^2}\cos\omega\right]^{-\frac{1}{2}} \tag{34}$$

is the normalization constant and $\alpha = r\mathrm{e}^{\mathrm{i}\delta}$ is a coherent state parameter with modulus r and argument δ. The normalized final state of the Schrödinger cat state after the postselected weak measurement is given by taking $|\phi\rangle = |\Theta\rangle$ in Eq. (6), i.e.,

$$|\chi\rangle = \frac{\kappa}{2}\left[(1+\langle A\rangle_{\mathrm{w}})D\left(\frac{s}{2}\right) + (1-\langle A\rangle_{\mathrm{w}})D\left(-\frac{s}{2}\right)\right]|\Theta\rangle \tag{35}$$

with the normalization coefficient

$$\begin{aligned}\kappa^{-2} =\ & \frac{1}{2}(1+|\langle A\rangle_{\mathrm{w}}|^2)+K^2(1-|\langle A\rangle_{\mathrm{w}}|^2)\cos(2s\,\mathrm{Im}[\alpha])\,\mathrm{e}^{-\frac{s^2}{2}} \\ & +\frac{K^2}{2}\mathrm{Re}[(1-\langle A\rangle_{\mathrm{w}})(1+\langle A\rangle_{\mathrm{w}}^*) \\ & \times(\mathrm{e}^{\mathrm{i}\omega}\,\mathrm{e}^{-\frac{1}{2}|2\alpha+s|^2}+\mathrm{e}^{-\mathrm{i}\omega}\,\mathrm{e}^{-\frac{1}{2}|2\alpha-s|^2})].\end{aligned} \tag{36}$$

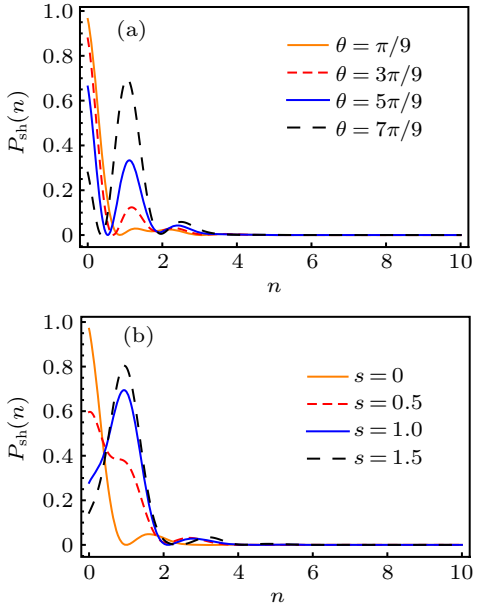

Fig. 7. Photon distribution $P_{\mathrm{sh}}(n)$ of the squeezed state as a function of photon number n. Here $\delta=\pi/3$, $\varphi=\pi/3$, $\omega=0$, $r=0.5$: (a) $P_{\mathrm{sh}}(n)$ is plotted for $s=1$, and for various weak values; (b) $P_{\mathrm{sh}}(n)$ is plotted for $\theta=7\pi/9$, and for various interaction strength s.

Here we must mention that $\omega\in[0,2\pi]$, and when $\omega=0$ ($\omega=\pi$) it is called the even (odd) Schrödinger cat state. Simi-

lar to the previous two cases, the conditional probability $P_{\rm sh}(n)$ of the Schrödinger cat state can be obtained by replacing the $|\phi\rangle$ in Eq. (5) to $|\chi\rangle$, and the analytical results of the even Schrödinger cat state is presented in Fig. 7. As shown in Fig. 7, the postselected measurement can change photon distribution of the field, and in fewer photon regions with large weak values, $P_{\rm sh}(n)$ is larger than the initial photon distribution of the Schrödinger even cat state. By comparing Fig. 7 and Fig. 4 we can also obtain the same common sense that the even Schrödinger cat state has similar properties as a squeezed state.

The Mandel factor and second-order correlation function for the Schrödinger cat state are given by

$$Q_{\rm m} = \frac{4|\alpha|^2 {\rm e}^{-2|\alpha|^2}\cos\omega}{1-{\rm e}^{-4|\alpha|^2}\cos^2\omega} \tag{37}$$

and

$$g^{(2)}(0) = 1 + \frac{4{\rm e}^{-2|\alpha|^2}\cos\omega}{(1-{\rm e}^{-2|\alpha|^2}\cos\omega)^2}, \tag{38}$$

respectively. It is apparent that both $g^{(2)}(0)$ and $Q_{\rm m}$ have sub-Poisson statistics when $\cos\omega < 0$ ($\frac{\pi}{2} < \omega < \frac{3\pi}{2}$).

The $g^{(2)}_{\rm sh}(0)$ and $Q_{\rm m,sh}$ of the Schrödinger cat state can be calculated using Eqs. (13) and (14) with the normalized final pointer state $|\chi\rangle$. As indicated in Fig. 8, after postselected measurement, the statistical property of the Schrödinger cat state changes from sub-Poisson to super-Poisson gradually with increasing the interaction strength and weak value. However, as we can see from Figs. 8(b) and 8(d), in the postselected weak measurement regime, where $0 < s < 1$, we can achieve the best performance for nonclassicality of the odd Schrödinger cat state with small coherent state modulus r.

The squeezing parameter of the initial Schrödinger cat state $|\Theta\rangle$ reads[47]

$$\begin{aligned} S^{in}_{\phi} = {} & \frac{|\alpha|^2{\rm e}^{-4|\alpha|^2}}{(1+{\rm e}^{-2|\alpha|^2}\cos\omega)^2} \\ & \times\big[1+\big(\cos 2\phi({\rm e}^{2|\alpha|^2}+\cos\omega)^2 \\ & +\sin^2\omega\cos^2\phi-1\big)\big]. \end{aligned} \tag{39}$$

From this expression, we can deduce that the squeezing effect of the initial Schrödinger cat state is also phase-dependent, similar to the squeezed vacuum state. The quadrature of the field will be squeezed only when the inequality $\cos 2\phi < \frac{\sin^2\omega\cos^2\phi-1}{(\cos\omega+{\rm e}^{2|\alpha|^2})^2}$ is satisfied. The details of this squeezing effect are presented in Fig. 9(a) (see the black solid curve).

The analytic expression of $S_{\phi,sch}$ for the Schrödinger cat state after postselected measurement can be achieved using the final normalized state $|\chi\rangle$, and the analytical results are summarized in Fig. 9. As indicated in Fig. 9, after postselected measurement, the squeezing effect of the Schrödinger cat state still depends on phase ϕ, and the squeezing effect of both the even and odd Schrödinger cat states are increased with increasing the interaction strength s and for small weak values (see Figs. 9(a), 9(b), and 9(d)). However, the odd Schrödinger cat pointer state has no squeezing effect (see Figs. 9(c) and 9(d)).

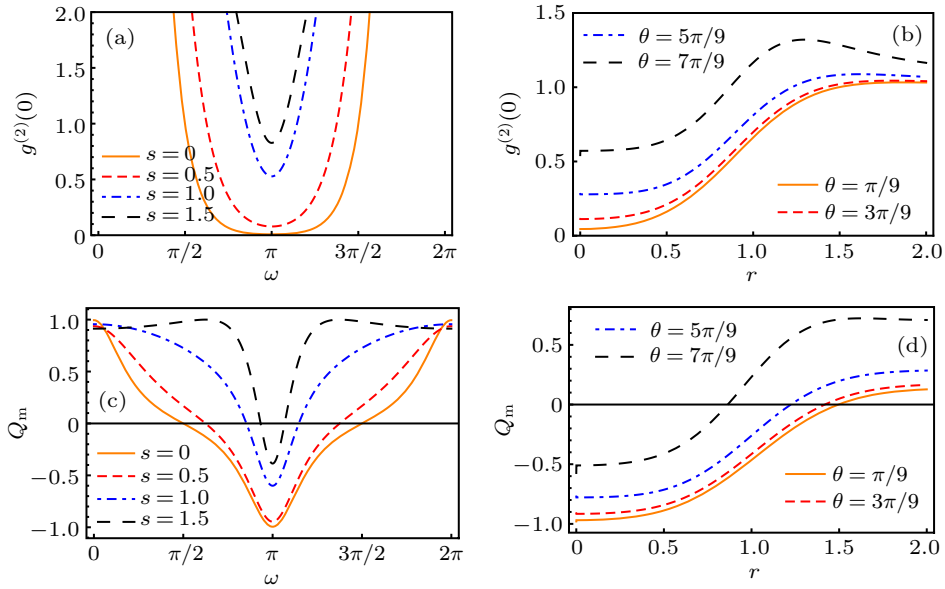

Fig. 8. Second-order correlation function $g^{(2)}_{\rm sh}(0)$ and Mandel factor $Q_{\rm m,sh}$ of the Schrödinger state after postselected measurement. Here $\varphi = 0$, $\delta = 0$: (a) $g^{(2)}_{\rm sh}(0)$ plotted as a function ω of the Schrödinger cat state for various interaction strength s and for $\theta = \pi/9$, $r = 0.3$; (b) $g^{(2)}_{\rm sh}(0)$ vs. parameter r of the Schrödinger cat state for different weak values and for $s = 0.5$, $\omega = \pi$; (c) $Q_{\rm m,sh}$ plotted as a function ω of the Schrödinger cat state for various interaction strength s and for $\theta = \pi/9$, $r = 0.3$; (d) $Q_{\rm m,sh}$ vs. parameter r of the Schrödinger cat state for different weak values and for $s = 0.5$, $\omega = \pi$.

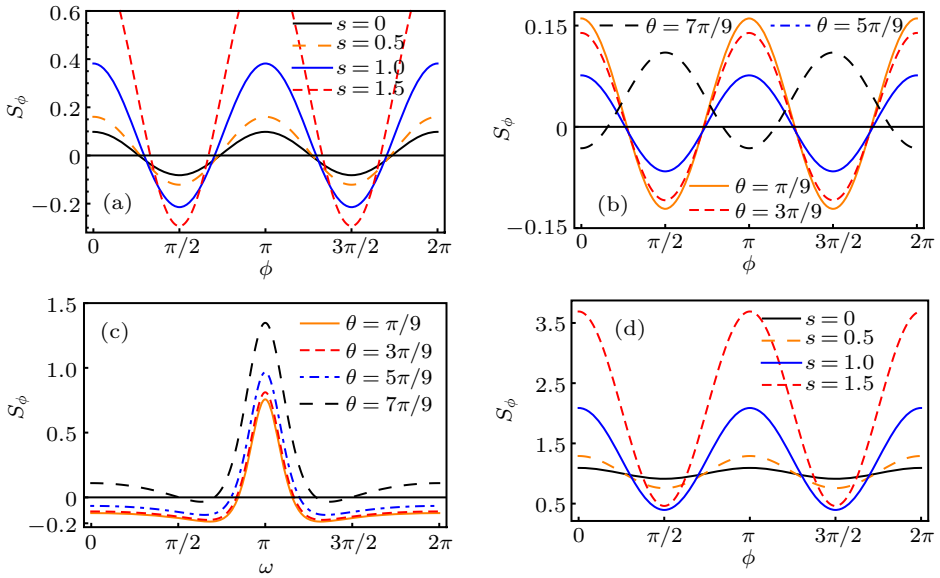

Fig. 9. Squeezing parameter $S_{\phi,\mathrm{sh}}$ of the Schrödinger cat state. Here $\varphi=0$, $\delta=0$, $r=0.3$. $S_{\phi,\mathrm{sh}}$ of the even Schrödinger cat state ($\omega=0$) vs. the squeezing parameter angle ϕ for different interaction strength and for $\theta=\pi/9$ in (a); for different weak values and for $s=0.5$ in (b). (c) $S_{\phi,\mathrm{sh}}$ plotted as a function of ω for various weak values and for $s=0.5$, $\phi=\pi/2$. (d) $S_{\phi,\mathrm{sh}}$ of the odd Schrödinger cat state ($\omega=\pi$) vs. the squeezing parameter angle ϕ for different interaction strength and for $\theta=\pi/9$.

4. Conclusion and remarks

In summary, we have investigated the effects of postselected measurement characterized by postselection and weak value on the statistical properties and squeezing effects of single-mode radiation fields. To achieve our goal, we take the coherent state, squeezed vacuum state and Schrödinger cat state as a pointer, and their polarization degrees of freedom as the measurement system, respectively. We have derived analytical expressions of the pointer state's normalized final state after postselected measurement considering all interaction strengths between the pointer and the measured system. We separately present the exact expressions of photon distributions, second-order correlation functions, Mandel factors and squeezing parameters of the above three typical single-mode radiation fields for the corresponding final pointer states, and plot the figures to analyze the results.

We find that the photon distributions of those three pointer states change significantly after postelected measurement, especially the coherent pointer state. It is shown that postselected measurement changes the photon statistics and squeezing effect of coherent state dramatically, and it is noticed that the amplification effect of weak value plays a major role in this process. We also show that the postselected measurement changes the photon statistics of the squeezed vacuum state from super-Poisson to sub-Poisson for large weak values, and moderate interaction strengths. However, the photon statistics of the Schrödinger cat state changes from sub-Poisson to super-Poisson with increasing the interaction strength. In accordance with previous findings, the squeezing effects of squeezed vacuum and Schrödinger cat pointer states are still phase-dependent and the squeezing effect of squeezed vacuum pointer is decreased with increasing the interaction strength. On the contrary, the squeezing effect of the even Schrödinger cat state is increased with increasing the interaction strength for small weak values compared with the initial pointer state case.

This work belongs to the state optimization using postselected von Neumann measurement. Those properties of radiation fields we investigated are directly effect on the implementations of the important quantum information processing mentioned in the introduction section. Thus, we anticipate that the results shown in this research can be useful to provide other effective methods for studying the related quantum information processing.

In our current research, we only consider the three typical single-mode radiation fields to investigate the effects of postselected von Neuman measurement on their inherent properties, but real light beams are in fact the time-dependent and the representation of time dependence requires the use of two or more modes of the optical systems. Thus, it would be interesting to check the effects of postselected von Neumann measurement on other useful radiation fields in quantum optics and quantum information processing such as single photon-added[58,59] and photon-subtracted[60] states, pair-coherent state (two-mode field),[61–64] and other multimode radiation fields.[65]

Appendix A: The explicit expressions of some quantities

(1) **For squeezed vacuum pointer state** The expectation value of photon number operator $a^\dagger a$ under the state $|\chi\rangle$ is

given by

$$\langle a^\dagger a\rangle_\varphi = \frac{|\kappa|^2}{4}\Big\{2(1+|\langle A\rangle_{\rm w}|^2)\Big(\frac{s^2}{4}+\sinh^2\eta\Big) + 2{\rm Re}\Big[(1-\langle A\rangle_{\rm w})(1+\langle A\rangle_{\rm w})^* I\Big]\Big\} \quad \text{(A1)}$$

with

$$I = \exp\Big[-\frac{s^2}{2}|\cosh\eta+{\rm e}^{{\rm i}\delta}\sinh\eta|^2\Big] \times\Big(\sinh^2\eta+\frac{s^2}{4}-\frac{s^2}{2}(1+i\sin\delta\sinh 2\eta)\Big).$$

In calculating the squeezing parameter, we use $\langle X_\phi\rangle_\varphi$ and $\langle X_\phi^2\rangle_\varphi$, and their expressions are given by

$$\begin{aligned}\langle X_\phi\rangle_\varphi = s\frac{|\kappa|^2}{4\sqrt{2}}\Big\{&\cos\phi|1+\langle A\rangle_{\rm w}|^2-\cos\phi|1+\langle A\rangle_{\rm w}|^2\\ &+2\exp\Big[-\frac{s^2}{2}|\cosh\eta+{\rm e}^{{\rm i}\delta}\sinh\eta|^2\Big]\\ &\times{\rm Re}\Big[{\rm e}^{-{\rm i}\theta}(1+\langle A\rangle_{\rm w})(1-\langle A\rangle_{\rm w})^*\\ &\times\Big(\cosh^2\eta+\frac{1}{2}{\rm e}^{{\rm i}\delta}\sinh 2\eta-\frac{1}{2}\Big)\Big]\\ &-2\exp\Big[-\frac{s^2}{2}|\cosh\eta+{\rm e}^{{\rm i}\delta}\sinh\eta|^2\Big]\\ &\times{\rm Re}\Big\{{\rm e}^{{\rm i}\theta}(1+\langle A\rangle_{\rm w})^*(1-\langle A\rangle_{\rm w})\\ &\times\Big[\cosh^2\eta+{\rm e}^{{\rm i}\delta}\frac{1}{2}\sinh 2\eta-\frac{1}{2}\Big]\Big\}\end{aligned}$$

$$\langle X_\theta^2\rangle = \frac{1}{2}[2{\rm Re}(II\,{\rm e}^{-2{\rm i}\phi})+2\langle a^\dagger a\rangle+1] \quad \text{(A2)}$$

with

$$\begin{aligned}II = \frac{|\kappa|^2}{4}\Big\{&\Big(\frac{s^2}{4}-\frac{1}{2}\sinh(2\eta){\rm e}^{-{\rm i}\delta}\Big)|1+\langle A\rangle_{\rm w}|^2\\ &+\Big(\frac{s^2}{4}-\frac{1}{2}\sinh(2\eta){\rm e}^{-{\rm i}\delta}\Big)|1-\langle A\rangle_{\rm w}|^2\\ &+(1-|\langle A\rangle_{\rm w}|^2)III\Big\},\end{aligned}$$

where

$$\begin{aligned}III = &\frac{s^2}{4}+s^2\Big(\frac{1}{2}{\rm e}^{-{\rm i}\delta}\sinh 2\eta+\sinh^2\eta\Big)\\ &+s^2(\cosh\eta+{\rm e}^{{\rm i}\delta}\sinh\eta)^2{\rm e}^{-2{\rm i}\delta}\sinh^2\eta\\ &-{\rm e}^{-{\rm i}\delta}\frac{1}{2}\sinh 2\eta\Big\}\exp\Big[-\frac{s^2}{2}|\cosh\eta+{\rm e}^{{\rm i}\delta}\sinh\eta|^2\Big].\end{aligned}$$

(2) **For Schrödinger cat pointer state** The expectation value of photon number operator $a^\dagger a$ and $a^{\dagger 2}a^2$ under the state $|\chi\rangle$ is given by

$$\begin{aligned}\langle a^\dagger a\rangle_\chi = \frac{|\kappa|^2K^2}{4}\Big\{&|1+\langle A\rangle_{\rm w}|^2\Big[|\alpha+\frac{s}{2}|^2+|-\alpha+\frac{s}{2}|^2+{\rm e}^{{\rm i}\omega}\Big(\alpha+\frac{s}{2}\Big)^*\\ &\times\Big(-\alpha+\frac{s}{2}\Big){\rm e}^{-2|\alpha|^2}+{\rm e}^{-{\rm i}\omega}\Big(-\alpha+\frac{s}{2}\Big)^*\Big(\alpha+\frac{s}{2}\Big){\rm e}^{-2|\alpha|^2}\Big]\\ &+|1-\langle A\rangle_{\rm w}|^2\Big[|\alpha-\frac{s}{2}|^2+|\alpha+\frac{s}{2}|^2-{\rm e}^{{\rm i}\omega}\Big(\alpha-\frac{s}{2}\Big)^*\Big(\alpha+\frac{s}{2}\Big){\rm e}^{-2|\alpha|^2}-{\rm e}^{-{\rm i}\omega}\Big(\alpha+\frac{s}{2}\Big)^*\Big(\alpha-\frac{s}{2}\Big){\rm e}^{-2|\alpha|^2}\Big]\\ &-2{\rm Re}\Big[\Big({\rm e}^{{\rm i}\omega}|\alpha+\frac{s}{2}|^2{\rm e}^{-2|\alpha+\frac{s}{2}|^2}+{\rm e}^{-{\rm i}\omega}{\rm e}^{-2|\alpha-\frac{s}{2}|^2}|\alpha-\frac{s}{2}|^2-2{\rm e}^{-\frac{s^2}{2}}\\ &\times{\rm Re}\Big[{\rm e}^{2{\rm i}s{\rm Im}(\alpha)}\Big(\alpha+\frac{s}{2}\Big)^*\Big(\alpha-\frac{s}{2}\Big)\Big]\Big)(1-\langle A\rangle_{\rm w})(1+\langle A\rangle_{\rm w})^*\Big]\Big\},\end{aligned} \quad \text{(A3)}$$

$$\begin{aligned}\langle a^{\dagger 2}a^2\rangle_\chi = \frac{|\kappa|^2K^2}{4}\{&|1+\langle A\rangle_{\rm w}|^2\Big[|\alpha+\frac{s}{2}|^4+|-\alpha+\frac{s}{2}|^4+{\rm e}^{{\rm i}\omega}\Big(\alpha^*+\frac{s}{2}\Big)^2\\ &\Big(-\alpha+\frac{s}{2}\Big)^2{\rm e}^{-2|\alpha|^2}+{\rm e}^{-{\rm i}\omega}\Big(-\alpha^*+\frac{s}{2}\Big)^2\Big(\alpha+\frac{s}{2}\Big)^2{\rm e}^{-2|\alpha|^2}\Big]\\ &+|1-\langle A\rangle_{\rm w}|^2\Big[|\alpha-\frac{s}{2}|^4+|\alpha+\frac{s}{2}|^4+{\rm e}^{{\rm i}\omega}{\rm e}^{-2|\alpha|^2}\Big(\alpha^*-\frac{s}{2}\Big)^2\Big(\alpha+\frac{s}{2}\Big)^2+{\rm e}^{-{\rm i}\omega}{\rm e}^{-2|\alpha|^2}\Big(\alpha^*+\frac{s}{2}\Big)\Big(\alpha-\frac{s}{2}\Big)^2\Big]\\ &+2{\rm Re}\Big[\Big({\rm e}^{{\rm i}\omega}|\alpha+\frac{s}{2}|^4{\rm e}^{-2|\alpha+\frac{s}{2}|^2}+{\rm e}^{-{\rm i}\omega}|\alpha-\frac{s}{2}|^4{\rm e}^{-2|\alpha-\frac{s}{2}|^2}\\ &+2{\rm e}^{-\frac{s^2}{2}}{\rm Re}\Big[{\rm e}^{2{\rm i}s{\rm Im}(\alpha)}(\alpha^*+\frac{s}{2})^2(\alpha-\frac{s}{2})^2\Big]\Big)(1-\langle A\rangle_{\rm w})(1+\langle A\rangle_{\rm w})^*\Big]\Big\}.\end{aligned} \quad \text{(A4)}$$

In calculation of the squeezing parameter, we use $\langle X_\phi\rangle_\chi$ and $\langle X_\phi^2\rangle_\chi$, and their expressions are given by

$$\langle X_\phi\rangle_\chi = \sqrt{2}{\rm Re}[\langle a\rangle_\chi{\rm e}^{-{\rm i}\phi}]$$

with

$$\begin{aligned}\langle a\rangle_\chi = \frac{|\kappa|^2K^2}{4}\Big\{&|1+\langle A\rangle_{\rm w}|^2[s+{\rm e}^{{\rm i}\phi}\left(-\alpha+\frac{s}{2}\right){\rm e}^{-2|\alpha|^2}+{\rm e}^{-{\rm i}\phi}\left(\alpha+\frac{s}{2}\right){\rm e}^{-2|\alpha|^2}]\\&+|1-\langle A\rangle_{\rm w}|^2\left[-s-{\rm e}^{{\rm i}\phi}\left(\alpha+\frac{s}{2}\right){\rm e}^{-2|\alpha|^2}+{\rm e}^{-{\rm i}\phi}\left(\alpha-\frac{s}{2}\right){\rm e}^{-2|\alpha|^2}\right]\\&+(1-\langle A\rangle_{\rm w})(1+\langle A\rangle_{\rm w})^*\Big[(2{\rm i}\alpha\sin(2s\,{\rm Im}[\alpha])-s\cos(2s\,{\rm Im}[\alpha]))\,{\rm e}^{-\frac{1}{2}s^2}\\&-{\rm e}^{{\rm i}\phi}\left(\alpha+\frac{s}{2}\right){\rm e}^{-\frac{1}{2}|2\alpha+s|^2}+{\rm e}^{-{\rm i}\phi}\left(\alpha-\frac{s}{2}\right){\rm e}^{-\frac{1}{2}|2\alpha-s|^2}\Big]\\&+(1-\langle A\rangle_{\rm w})^*(1+\langle A\rangle_{\rm w})\Big[(-2{\rm i}\alpha\sin(2s\,{\rm Im}[\alpha])+s\cos(2s\,{\rm Im}[\alpha]))\,{\rm e}^{-\frac{1}{2}s^2}\\&+{\rm e}^{{\rm i}\phi}\left(-\alpha+\frac{s}{2}\right){\rm e}^{-\frac{1}{2}|2\alpha-s|^2}+{\rm e}^{-{\rm i}\phi}\left(\alpha+\frac{s}{2}\right){\rm e}^{-\frac{1}{2}|2\alpha+s|^2}\Big]\Big\},\end{aligned}$$

$$\langle X_\phi^2\rangle_\chi = \frac{1}{2}[2\langle a^\dagger a\rangle_\chi + 2{\rm Re}[\langle a^2\rangle_\chi {\rm e}^{-2{\rm i}\phi}]+1],$$

with

$$\begin{aligned}\langle a^2\rangle_\chi = \frac{|\kappa|^2K^2}{4}\Big\{&|1+\langle A\rangle_{\rm w}|^2\left[2(\alpha^2+\frac{s^2}{4})+{\rm e}^{{\rm i}\omega}{\rm e}^{-2|\alpha|^2}\left(-\alpha+\frac{s}{2}\right)^2+{\rm e}^{-{\rm i}\omega}{\rm e}^{-2|\alpha|^2}\left(\alpha+\frac{s}{2}\right)^2\right]\\&+|1-\langle A\rangle_{\rm w}|^2\left[2(\alpha^2+\frac{s^2}{4})+{\rm e}^{{\rm i}\omega}{\rm e}^{-2|\alpha|^2}\left(\alpha+\frac{s}{2}\right)^2+{\rm e}^{-{\rm i}\omega}{\rm e}^{-2|\alpha|^2}\left(\alpha-\frac{s}{2}\right)^2\right]\\&+(1-\langle A\rangle_{\rm w})(1+\langle A\rangle_{\rm w})^*\Big[2{\rm e}^{-\frac{s^2}{4}}(\cos(2s\,{\rm Im}[\alpha])\left(\alpha^2+\frac{s^2}{4}\right)-{\rm i}s\alpha\sin(2s\,{\rm Im}[\alpha]))\\&+{\rm e}^{-{\rm i}\omega}\left(\alpha-\frac{s}{2}\right)^2{\rm e}^{-2|\alpha-\frac{s}{2}|^2}+{\rm e}^{{\rm i}\omega}\left(\alpha+\frac{s}{2}\right)^2{\rm e}^{-2|\alpha+\frac{s}{2}|^2}\Big]\\&+(1+\langle A\rangle_{\rm w})(1-\langle A\rangle_{\rm w})^*\Big[2{\rm e}^{-\frac{s^2}{4}}(\cos(2s\,{\rm Im}[\alpha])\left(\alpha^2+\frac{s^2}{4}\right)-{\rm i}s\alpha\sin(2s\,{\rm Im}[\alpha]))\\&+{\rm e}^{{\rm i}\omega}\left(\alpha-\frac{s}{2}\right)^2{\rm e}^{-2|\alpha-\frac{s}{2}|^2}+{\rm e}^{-{\rm i}\omega}\left(\alpha+\frac{s}{2}\right)^2{\rm e}^{-2|\alpha+\frac{s}{2}|^2}\Big]\Big\}.\end{aligned}\tag{A5}$$

References

[1] Aharonov Y, Albert D Z and Vaidman L 1988 *Phys. Rev. Lett.* **60** 1351
[2] von Neumann J 1955 *Mathematical Foundations of Quantum Mechanics* (Princeton: Princeton University Press) p. 91
[3] Ritchie N, Story J and Hulet R 1991 *Phys. Rev. Lett.* **66** 1107
[4] Kofman A G, Ashhab S and Nori F 2012 *Phys. Rep.* **520** 43
[5] Dressel J, Malik M, Miatto F M, Jordan A N and Boyd R W 2014 *Rev. Mod. Phys.* **86** 307
[6] Aharonov Y and Botero A 2005 *Phys. Rev. A* **72** 052111
[7] Di Lorenzo A and Egues J C 2008 *Phys. Rev. A* **77** 042108
[8] Pan A K and Matzkin A 2012 *Phys. Rev. A* **85** 022122
[9] Nakamura K, Nishizawa A and Fujimoto M K 2012 *Phys. Rev. A* **85** 012113
[10] Turek Y, Kobayashi H, Akutsu T, Sun C P and Shikano Y 2015 *New J. Phys.* **17** 083029
[11] de Lima Bernardo B, Azevedo S and Rosas A 2014 *Opt. Commun.* **331** 194
[12] Turek Y, Maimaiti W, Shikano Y, Sun C P and Al-Amri M 2015 *Phys. Rev. A* **92** 022109
[13] Pang S and Brun T A 2015 *Phys. Rev. Lett.* **115** 120401
[14] Turek Y and Yusufu T 2018 *Eur. Phys. J. D* **72** 202
[15] Kedem Y and Vaidman L 2010 *Phys. Rev. Lett.* **105** 230401
[16] Buller G S and Collins R J 2010 *Meas. Sci. Technol.* **21** 12002
[17] Khalili F Y, Miao H and Chen Y 2009 *Phys. Rev. D* **80** 042006
[18] Grote H, Weinert M, Adhikari R X, Affeldt C and Wittel H 2016 *Opt. Express* **24** 20107
[19] Braunstein S L and Kimble H J 1998 *Phys. Rev. Lett.* **80** 869
[20] Milburn G J and Braunstein S L 1999 *Phys. Rev. A* **60** 937
[21] Jeong H, Kim M S and Lee J 2001 *Phys. Rev. A* **64** 052308
[22] van Enk S J and Hirota O 2001 *Phys. Rev. A* **64** 022313
[23] Ralph T C, Gilchrist A, Milburn G J, Munro W J and Glancy S 2003 *Phys. Rev. A* **68** 042319
[24] Muschik C A, Hammerer K, Polzik E S and Cirac J I 2006 *Phys. Rev. A* **73** 062329
[25] Li L, Dudin Y O and Kuzmich A 2013 *Nature* **498** 466
[26] Hacker B, Welte S, Daiss S, Shaukat A, Ritter S, Li L and Rempe G 2019 *Nat. Photon.* **13** 110
[27] Munro W J, Nemoto K, Milburn G J and Braunstein S L 2002 *Phys. Rev. A* **66** 023819
[28] Glauber R J 1963 *Phys. Rev.* **131** 2766
[29] Carranza R and Gerry C C 2012 *J. Opt. Soc. Am. B* **29** 2581
[30] Andersen U L, Gehring T, Marquardt C and Leuchs G 2016 *Phys. Scripta* **91** 053001
[31] Monroe C, Meekhof D M, King B E and Wineland D J 1996 *Science* **272** 1131
[32] Ourjoumtsev A, Jeong H, Tualle-Brouri R and Grangier P 2007 *Nature* **448** 784
[33] Haroche S 2013 *Rev. Mod. Phys.* **85** 1083
[34] Starling D J, Dixon P B, Jordan A N and Howell J C 2009 *Phys. Rev. A* **80** 041803
[35] Hosten O and Kwiat P 2008 *Science* **319** 787
[36] Dixon P B, Starling D J, Jordan A N and Howell J C 2009 *Phys. Rev. Lett.* **102** 173601
[37] Zhou L, Turek Y, Sun C P and Nori F 2013 *Phys. Rev. A* **88** 053815
[38] Starling D J, Dixon P B, Jordan A N and Howell J C 2010 *Phys. Rev. A* **82** 063822

[39] Magaña Loaiza O S, Mirhosseini M, Rodenburg B and Boyd R W 2014 *Phys. Rev. Lett.* **112** 200401
[40] Pfeifer M and Fischer P 2011 *Opt. Express* **19** 16508
[41] de Lima Bernardo B, Azevedo S and Rosas A 2014 *Phys. Lett. A* **378** 2029
[42] Viza G I, Martínez-Rincón J, Howland G A, Frostig H, Shomroni I, Dayan B and Howell J C 2013 *Opt. Lett.* **38** 2949
[43] Egan P and Stone J A 2012 *Opt. Lett.* **37** 4991
[44] Aharonov Y and Rohrlich D 2005 *Quantum Paradoxes-Quantum Theory for the Perplexed* (Weinheim: Wiley-VCH) p. 124
[45] Gerry C and Knight P 2005 *Introductory Quantum Optics* (Cambridge: Cambridge University Press) p. 90
[46] Mandel L 1979 *Opt. Lett.* **4** 205
[47] Agarwal G 2013 *Quantum Optics* (Cambridge: Cambridge University Press) p. 230
[48] Schrödinger E 1926 *Naturwissenschaften* **14** 664
[49] Klauder J and Skagerstam B 1985 *Coherent States* (Singpore: World Scientific) p. 134
[50] Perelomov 1986 *Generalized Coherent States and Their Applications* (Berlin: Springer) p. 254
[51] Scully M and Zubairy M 1997 *Quantum Optics* (Cambridge: Cambridge University Press) p. 24
[52] Wu L A, Kimble H J, Hall J L and Wu H 1986 *Phys. Rev. Lett.* **57** 2520
[53] Schrödinger E 1935 *Naturwissenschaften* **23** 807
[54] Sanders B C 1992 *Phys. Rev. A* **45** 6811
[55] Wenger J, Hafezi M, Grosshans F, Tualle-Brouri R and Grangier P 2003 *Phys. Rev. A* **67** 012105
[56] Jeong H, Son W, Kim M S, Ahn D and Brukner C 2003 *Phys. Rev. A* **67** 012106
[57] Stobińska M, Jeong H and Ralph T C 2007 *Phys. Rev. A* **75** 052105
[58] Zavatta A, Viciani S and Bellini M 2004 *Science* **306** 660
[59] Barbieri M, Spagnolo N, Genoni M G, Ferreyrol F, Blandino R, Paris M G A, Grangier P and Tualle-Brouri R 2010 *Phys. Rev. A* **82** 063833
[60] Biswas A and Agarwal G S 2007 *Phys. Rev. A* **75** 032104
[61] Agarwal G S 1988 *J. Opt. Soc. Am. B* **5** 1940
[62] Xin Z Z, Wang D B, Hirayama M and Matumoto K 1994 *Phys. Rev. A* **50** 2865
[63] Xin Z Z, Duan Y B, Zhang H M, Hirayama M and itiMatumoto K 1996 *J. Phys. B: At. Mol. Opt. Phys.* **29** 4493
[64] Yuen H 1976 *Phys. Rev. A* **13** 2226
[65] Blow K, Loudon R, Phoenix S and Shepherd T 1990 *Phys. Rev. A* **42** 4102